Discharge measurements at Chievo Dam power plant using 24 ultrasonic paths (IGHEM 2012)

J. Lanzersdorfer[1]
ANDRITZ Hydro GmbH, Ostring 17, 4031 Linz, Austria

Abstract

This paper deals with the discharge measurements on the module at Chievo Dam in Verona, Italy, which consists of 5 HYDROMATRIX® turbine-generator units. This test session took place in 2011.
The major challenge was to obtain reliable values of the discharge. It was decided to apply acoustic transit time (ATT) being aware of the fact that the inflow conditions were not consistent with IEC recommendations. 24 ultrasonic paths were installed in the open channel fulfilling the ambitious target concerning the measuring uncertainty ($\pm 2 \ldots 3\%$). Four (4) vertical frames were mounted on the side walls upstream the trash rake. Each one of the frames was equipped with 12 sensors. The average uncertainty of the total flow is estimated to be $\pm 2.3\%$. Finally, a criterion is introduced to quantify the required number of samples to undergo a maximum allowable random uncertainty of the main flow velocity.

Introduction

Since no major excavations or civil works are necessary, the HYDROMATRIX® turbine-generator concept represents an interesting and cheap hydro-power variant at low heads. Due to their small dimensions such units can easily be integrated into existing dam or gate structures. At Chievo Dam, the distinctive feature is that the complete module is installed into the existing lock chamber at its downstream end and can be lifted and lowered (under balanced condition) in order to evacuate the lock chamber for flood release. This module is equipped with five (5) turbine-generator units (TG units) with horizontal runner axis. The runner has a diameter of 1.32 m and three (3) non-movable blades. The blades are encircled by a metal ring which is equipped with permanent magnets. This represents the generator's rotor part. The stator of the generator is installed around that rotating ring. Fixed wicket gates are located upstream the runner. A vertically moveable gate downstream the short draft tube cone is used to start and stop the unit, and to synchronize the unit to the grid. In 2009 the HYDROMATRIX® module at Chievo Dam/Italy has been commissioned successfully by ANDRITZ Hydro.

In January 2011 efficiency measurements were carried out at Chievo Dam by measurement engineers from ANDRITZ Hydro. The target of this test session was to determine the performance characteristics of the module for different gross heads ($2.0 \ldots 3.6$ m). The only appropriate location where such measurements could be executed was upstream the trash rake in the open channel. The cross sectional shape of the channel represents a rectangle. The width is nearly 12.5 m, the maximum water depth 6 m. No applicable absolute measuring method consistent with IEC 60041 [1] – i.e. current meters – was satisfying. As far as the financial aspect was concerned, the application of current-meters

[1] Contact: johannes.lanzersdorfer@andritz.com

would have required at least 100 propellers which was inappropriate. Tracer-dilution measurements would have been strongly biased by deadwater regions and recirculation zones. As a consequence of this, it was decided to apply acoustic transit time (ATT) keeping in mind that the inflow conditions were not consistent with IEC recommendations. 24 ultrasonic paths were installed in the open channel. Velocity profile and discharge evaluations are carried out in accordance with ISO 6416:2004 [2].

Setup of the acoustic measurements

General aspects

The intake upstream the TG units has a vertical gate which could be lowered during installation works. Unfortunately, it was leaking and the water level downstream the closed gate could only be lowered to tailrace level if required. A few meters downstream that gate a fish ladder was built on the right-hand side. Following the main flow after the entrance to the fish ladder the hydraulic contour is a little bite broadened to the left-hand side. And a sharp vertical wall edge appears on the right before entering a short straight part. This flow guidance results in visible turbulences and vortices. Discharge measurements can only be performed reasonably just upstream the module in a short, straight and rectangular shaped part of the intake (width is nearly 12.5 m, the maximum water depth 6 m). The maximum average flow velocity yields approximately 0.75 m/s. Accurate measurement of such small velocities represent another challenge in a metrological point of view.

The conditions for ATT measurements on that site were not the best and recommendations from the standard test code [1] (straight intake with minium length of $10 \cdot D$, minimum velocity ≥ 1.5 m/s) could not be established. Despite this fact, the ambitious plan was made to use 24 acoustic paths arranged in crossed position to eliminate the main cross-flow. Locally disturbed flow within the measuring section which could not be detected by both paths of the same elevation is considered by additional uncertainty. The whole channel with set intake gate could not be emptied without additional financial efforts. Hence, it was decided to use a setup with four (4) vertical frames mounted on the side walls instead of installing each ultrasonic transducer individually on the walls.

Instrumentation and equipment

We used our equipment from ACCUSONIC for ATT measurements containing the main processor unit 7500 and two (2) additional 7520 units. Each of these units was equipped with 8 transducer pairs. These electronic devices were put into a container of 10' length just next to the intake. 48 ultrasonic sensors of type 7618 were used. Those work with a ultrasonic frequency of 500 kHz and are suitable for conduits up to 25 m wide [3]. The ball-type transducers can be adjusted on a protective mount. The connection between processor unit and transducer was made by special cables with waterproof plugs and a length of 60 m.

The raw data (the forth and back transit times of each path) were sent with an update rate of 1/3 Hz via RS232 connection to a laptop. The sampling time was set to 5 min yielding to 100 observations per measuring point. A selfmade software written in NI LabView took care of the data recording and the real-time analysis. The detailed analysis was executed with Excel including outlier filtering with the Grubbs test [1].

Installation of sensor frames

The frames were made of u-beams with 260 mm width. The ground plate where the sensors were mounted on had been finely machined to reduce any angular curvature. Opposite to the ground plate a few plates were welded onto the bars which served as buttstraps.

The frames were transported to the site after manufacturing. In detail, equipping the frames with sensors – 12 sensors per frame – and the cabling had to be done on site too. In order to determine the flow behavior close to the bottom as good as possible, the sensors on the frame were arranged in an appropriate vertical position. The lowest path elevation required a minimum distance to the bottom to avoid interference with reflected ultrasonic waves.[2] The same was valid for acoustic paths next to the expected headwater level. The path angle of each sensor with respect to the main flow was adjusted outside the channel and it yielded $\theta \cong 60°$. That proceeding was required since at least sensor pairs below tailrace level could not be aligned properly. But this default setting should ensure a good operation of the system despite the incorrect alignment. Because the main energy of the ultrasonic pulse is propagating within an angle of aperature of $\pm 5°$ [4]. The cables were guided in the hollow space of the u-beam.

A mobile crane hoisted the ready equipped frames into the intake channel where the water level was lowered to tailrace level. Each frame was mounted at its buttstraps onto the side wall with several anchor bolts. The construction of the frames and their fixation on the walls avoided any remarkable vibrations. The acoustic signals remained stable during the whole measuring session. The protrusion of the sensors on the frames into the channel were approximatey 15 to 20 cm depending on the structure of the side wall. The distance was quite

[2]The determination of the arrival time of the incoming ultrasonic pulse on an opposite transducer is mainly done by detecting the first full period of this pulse. Any reflected pulse would interfere with the signal of interest. Hence, it is necessary that the distance between any surface/bottom and its neighbored acoustic path do not go below $z_{\min}$. This parameter can be calculated by the aid of the minimium required phase difference λ between normal pulse and reflected pulse

$$\lambda = \sqrt{L^2 + (2z_{\min})^2} - L \tag{1}$$

where L denotes the shortest distance between opposite transducers. Transforming (1) and $\lambda = c/\nu$ yields

$$z_{\min} = \sqrt{\frac{Lc}{2\nu} + \left(\frac{c}{2\nu}\right)^2} \cong \sqrt{\frac{Lc}{2\nu}} \tag{2}$$

ν represents the pulse frequency. In case of the measurements at Chievo Dam the minimum distance may be estimated by

$$z_{\min} \cong \sqrt{\frac{(12.5\text{ m})/\sin(60°)\cdot(1450\text{ m/s})}{2\cdot(5\cdot 10^5\text{ Hz})}} \cong 0.15\text{ m} \tag{3}$$

small compared to the channel width of 12.5 m.
The position of the individual sensors above the water level was determined by means of a laser based distance measuring device. The geometric arrangement of the non-accessible sensors was obtained by extrapolation and statistics.

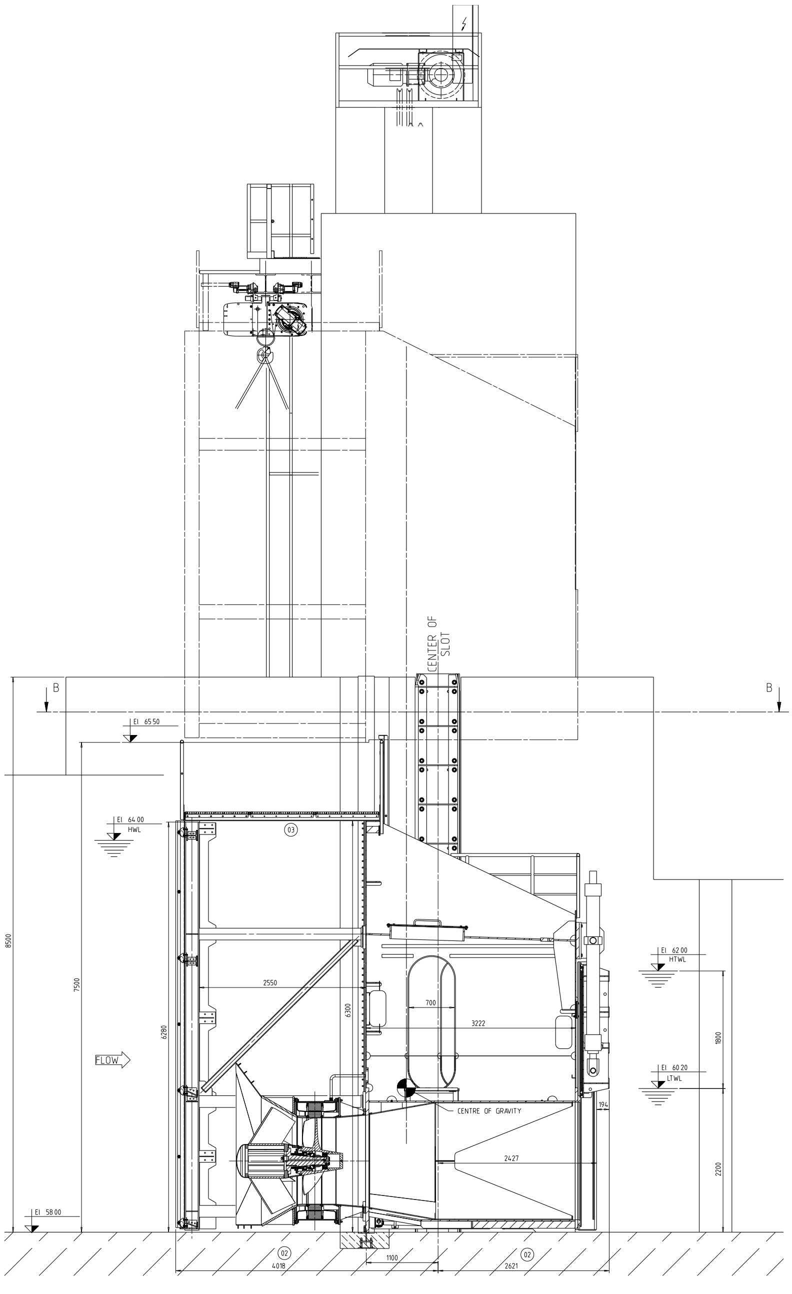

Figure 1: General layout of the HYDROMATRIX® module (sectional view)

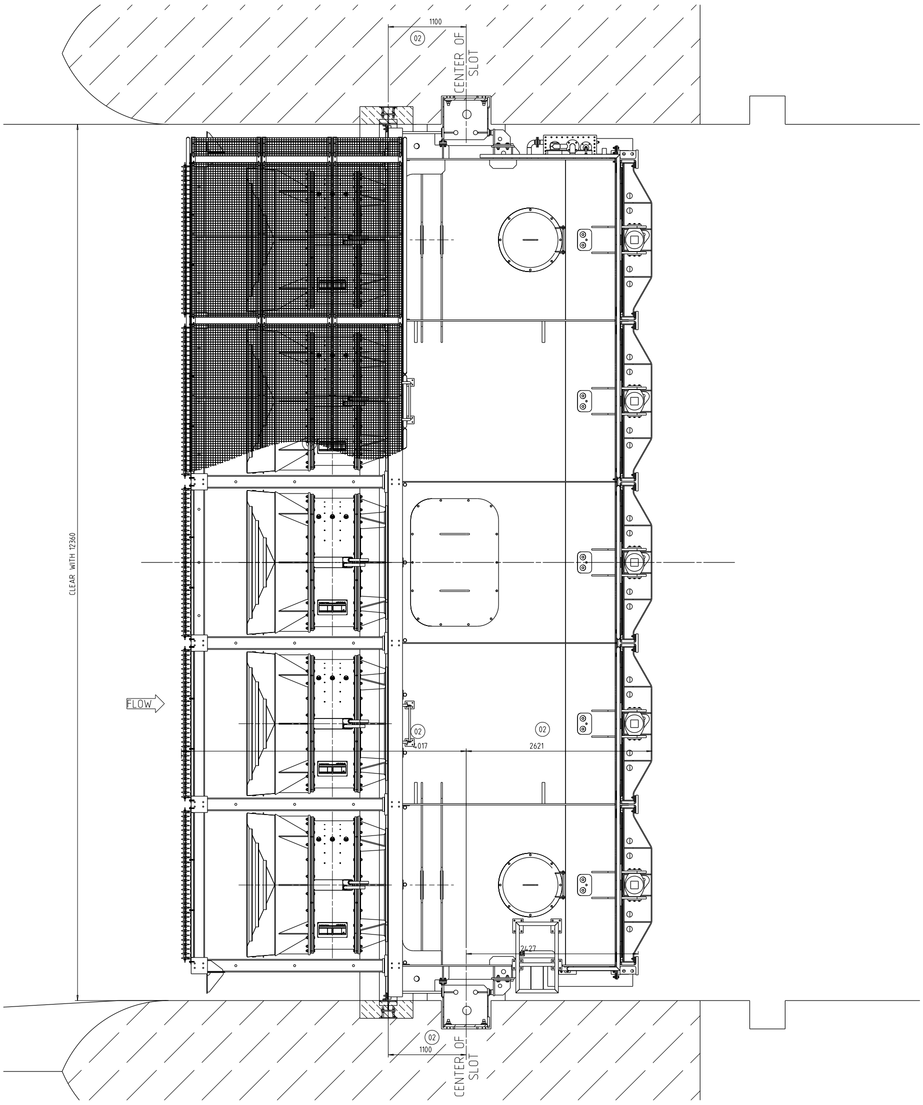

Figure 2: General layout of the HYDROMATRIX® module (plan view)

(a) View of the lifted module from the upstream side. The fish ladder is located on the right-hand side.

(b) View of the exit gates of the TG units

Figure 3: HYDROMATRIX® module during commissioning

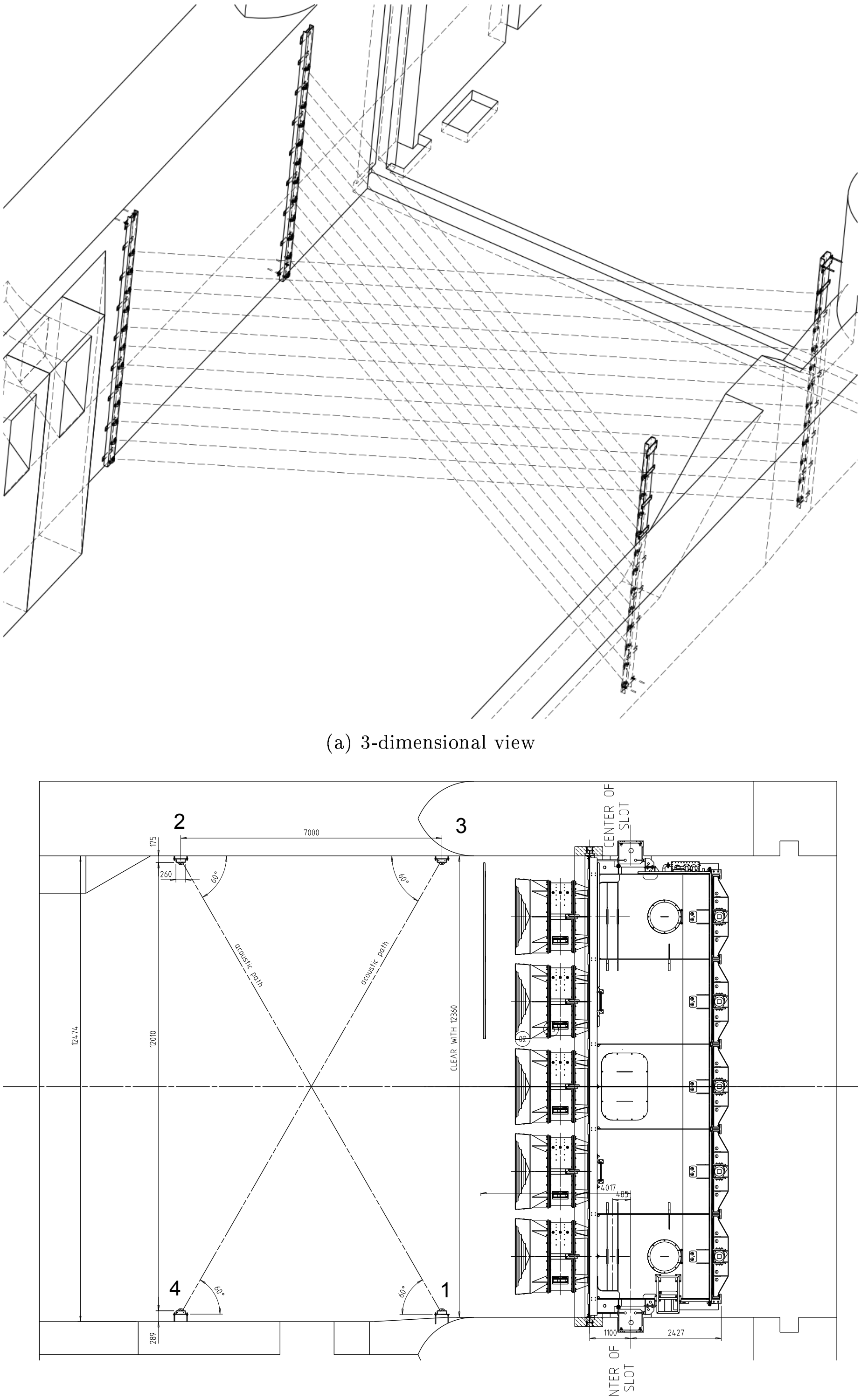

(a) 3-dimensional view

(b) Plan view

Figure 4: Scheme of the acoustic path arrangement

(a) Sensor mounting ($\theta = 60°$) and cabling outside the channel

(b) Mounted frames inside the intake channel: The water level in the intake part is equilibrated with the tailrace level. It was not possible to adjust sensor pairs with a laser below the water surface.

Figure 5: Installation of the sensor frames into the intake

Theory

Velocity calculation

The superposition of individual velocities in the flow at a certain elevation gives the basic formulae yielding to

$$\frac{L_1}{t_{1-2}} = c - \bar{v} \cdot \cos\theta_1 - \bar{v}_\perp \cdot \sin\theta_1 \tag{4}$$

$$\frac{L_1}{t_{2-1}} = c + \bar{v} \cdot \cos\theta_1 + \bar{v}_\perp \cdot \sin\theta_1 \tag{5}$$

$$\frac{L_2}{t_{3-4}} = c - \bar{v} \cdot \cos\theta_2 + \bar{v}_\perp \cdot \sin\theta_2 \tag{6}$$

$$\frac{L_2}{t_{4-3}} = c + \bar{v} \cdot \cos\theta_2 - \bar{v}_\perp \cdot \sin\theta_2 \tag{7}$$

$L_1, L_2 \ldots$ minimum path length of path 1 (sensor pair 1–2) and path 2 (sensor pair 3–4)
$t_{\mathrm{i-j}} \ldots$ transit time of ultrasonic pulse propagating from sensor i to sensor j
$\theta_i \ldots$ angle between path i and main flow direction
$\bar{v} \ldots$ axial flow velocity (positive sign corresponds to downstream direction)
$\bar{v}_\perp \ldots$ main cross flow velocity (positive sign corresponds to flow to the right when looking downstream)
c sonic sound in water (depending on temperature, pressure, chemical admixture)

Equations (4) to (7) represent an over-determined system of equations and, hence, no exact solution exists. However, it is possible to find estimates of the unknown parameters by linear regression analysis. Rewriting the equations above in matrix notation yields

$$\mathbf{y} = \mathbf{A} \cdot \mathbf{x} \tag{8}$$

with

$$\mathbf{y} = \begin{pmatrix} \frac{L_1}{t_{1-2}} & \frac{L_1}{t_{2-1}} & \frac{L_2}{t_{3-4}} & \frac{L_2}{t_{4-3}} \end{pmatrix}^T \tag{9}$$

$$\mathbf{A} = \begin{pmatrix} 1 & -\cos\theta_1 & -\sin\theta_1 \\ 1 & +\cos\theta_1 & +\sin\theta_1 \\ 1 & -\cos\theta_2 & +\sin\theta_2 \\ 1 & +\cos\theta_2 & -\sin\theta_2 \end{pmatrix} \tag{10}$$

$$\mathbf{x} = \begin{pmatrix} c & \bar{v} & \bar{v}_\perp \end{pmatrix}^T \tag{11}$$

Employing an equiweighted[3] regression delivers

$$\mathbf{x} = \left(\mathbf{A}^T\mathbf{A}\right)^{-1} \cdot \mathbf{A}^T \cdot \mathbf{y} \tag{12}$$

[3] Because absolute uncertainties of y-values do not differ significantly in real measurements.

or expressing the obtained regressors in individual equations, respectively,

$$c = \frac{L_1}{4} \cdot \left(\frac{1}{t_{1-2}} + \frac{1}{t_{2-1}} \right) + \frac{L_2}{4} \cdot \left(\frac{1}{t_{3-4}} + \frac{1}{t_{4-3}} \right) \tag{13}$$

$$\bar{v} = \frac{\tan\theta_2 \cdot v_1 + \tan\theta_1 \cdot v_2}{\tan\theta_1 + \tan\theta_2} \tag{14}$$

$$\bar{v}_\perp = \frac{v_1 - v_2}{\tan\theta_1 + \tan\theta_2} \tag{15}$$

where v_1 and v_2 denote the individual calculations of the axial velocities with respect to each acoustic transducer pair:

$$v_1 = \frac{L_1}{2\cos\theta_1} \cdot \left(\frac{1}{t_{2-1}} - \frac{1}{t_{1-2}} \right) \tag{16}$$

$$v_2 = \frac{L_2}{2\cos\theta_2} \cdot \left(\frac{1}{t_{4-3}} - \frac{1}{t_{3-4}} \right) \tag{17}$$

Discharge calculation

The calculations above result in $k = 12$ values of main flow velocities $\bar{v}_i \equiv \bar{v}(z_i)$ at different elevations z_i. The flow velocities at the bottom $\bar{v}_\mathrm{b}$ and on the surface $\bar{v}_\mathrm{s}$ need to be estimated. Therefore the procedure described in [2] is used. Although the bottom velocity is zero *per definitionem*, a fraction of the calculated velocity close to the bottom is used (typically $k_\mathrm{b} = 0.5$). The velocity value at the water surface may be obtained by extrapolation.

The total discharge may be calculated by integrating the velocity profile using Cartesian coordinates

$$Q = \int_{x_1}^{x_2} dx \int_{z_1}^{z_2} dz\, v(x,z) = \int_{z_1}^{z_2} dz\, w(z) \cdot \bar{v}(z) \tag{18}$$

where $w(z)$ and $\bar{v}(z)$ denote the channel width and the mean axial velocity at elevation z. Using a discrete number of elevations (nodes) changes the integral sign into a sum sign yielding

$$\begin{aligned} Q &\cong \sum_i (z_{i+1} - z_i) \cdot \frac{w_i + w_{i+1}}{2} \cdot \frac{\bar{v}_i + \bar{v}_{i+1}}{2} \\ &= \frac{1}{4} \cdot \sum_i (z_{i+1} - z_i) \cdot [w_i + w_{i+1}] \cdot [\bar{v}_i + \bar{v}_{i+1}] \end{aligned} \tag{19}$$

The number and the choice of nodes at distinct elevations may be done by experience.[4] Since the shape of flow profiles possesses higher gradients close to

[4] A special case occurs when the water level can be kept constant. Then the nodes may be chosen that way to allow discharge calculation similar to ATT measurements in closed conduits using Gaussian quadrature methods [5].

solid phase transitions a denser arrangement of acoustic paths in that region is recommended.
For the discharge evaluation at Chievo Dam the following formula is used

$$Q = Q_\mathrm{b} + Q_\mathrm{int} + Q_\mathrm{s} \tag{20}$$

With the bottom discharge

$$Q_\mathrm{b} = (z_1 - z_\mathrm{b}) \cdot w \cdot \bar{v}_1 \cdot \frac{1 + k_\mathrm{b}}{2} \tag{21}$$

the intermediate proportion

$$Q_\mathrm{int} = \frac{w}{2} \cdot \sum_{i=1}^{p} (z_{i+1} - z_i) \cdot [\bar{v}_i + \bar{v}_{i+1}] \tag{22}$$

and the surface discharge

$$Q_\mathrm{s} = (z_\mathrm{s} - z_p) \cdot w \cdot \frac{k_\mathrm{s} \cdot \bar{v}_\mathrm{s} + \bar{v}_p}{k_\mathrm{s} + 1} \tag{23}$$

The index p is equal to the elevation number of the highest lying and active paths, i.e. $p = k = 12$ at maximum intake level. The velocity at water surface $\bar{v}_\mathrm{s}$ is obtained by extrapolation but is limited to

$$\bar{v}_\mathrm{s} = \bar{v}_p + (\bar{v}_p + \bar{v}_{p-1}) \qquad \text{if} \quad (z_\mathrm{s} - z_p) > (z_p - z_{p-1}) \tag{24}$$

The constant $k_\mathrm{s} = 0.5$ represents a weighting factor of the surface velocity.

Uncertainty estimation

Velocity (regression regressors) The standard deviation of the chosen model functions (4) to (7) may be obtained by calculating

$$s_y = \sqrt{\frac{1}{n-m} \left(\mathbf{y}^T - \mathbf{x}^T \mathbf{A}^T\right) (\mathbf{y} - \mathbf{A}\mathbf{x})} \tag{25}$$

with the number of equations within the system of equations $n = 4$ and the number of regressors $m = 3$. The covariance of the contributing regressors r_i yields

$$\mathrm{Cov}(r_i, r_j) = s_y^2 (\mathbf{A}^T \mathbf{A})^{-1} \tag{26}$$

That is, the *random*[5] uncertainty of a regressor yields using the Student t-value $t = 12.7$ for 95 % confidence level and $n - m$ degrees of freedom

[5]This proportion of uncertainty to the total uncertainty of a regressor is of random type since its standard deviation is proportional to the inverse of the square root of the number of *observations* n:

$$s_{r_i} = \sqrt{\mathrm{Cov}(r_i, r_i)} = \sqrt{\mathrm{Var}(r_i)} \propto \frac{1}{\sqrt{n}} \tag{27}$$

$$e_{\mathrm{r}}(r_i) = \pm t \cdot \sqrt{\mathrm{Cov}(r_i, r_i)} \tag{28}$$

The total uncertainty of such a regressor is then obtained in the common way

$$e(r_i) = \pm\sqrt{e_{\mathrm{r}}^2(r_i) + e_{\mathrm{s}}^2(r_i)} \tag{29}$$

where $e_{\mathrm{s}}(r_i)$ denotes the *systematic* uncertainty of the regressor obtained by uncertainty propagation.

Discharge The uncertainty estimation of the flow Q is mainly affected by the uncertainty of the flow profile versus elevation. That is, using common uncertainty propagation for equations (21), (22) and (23) would lead to false and underestimated values. The impact of the integration in equation (18) with respect to the z-axis may be derived by

$$e(Q) = \pm\sqrt{\left[f(z_2 - z_1)\cdot Q\right]^2 + \left[\int_{z_1}^{z_2} dz\ \bar{v}(z)\cdot e(w(z))\right]^2 + \left[\int_{z_1}^{z_2} dz\ w(z)\cdot e(\bar{v}(z))\right]^2} \tag{30}$$

Here, the first term on the right-hand side considers the uncertainty of the integration limits (relative uncertainty $f(z_2 - z_1)$). The uncertainties of the intermediate elevations may be neglected. The second term is related to the channel's width, and the last one to the velocity profile. One obtains in the discrete case that

$$\begin{aligned} e(Q) \quad = \quad & \pm\Bigg\{\left[\frac{e^2(z_p) + e^2(z_1)}{(z_p - z_1)^2}\cdot Q^2\right] \\ & + \left[\frac{1}{4}\cdot\sum_i (z_{i+1} - z_i)\cdot(\bar{v}_i + \bar{v}_{i+1})\cdot(e(w_i) + e(w_{i+1}))\right]^2 \\ & + \left[\frac{1}{4}\cdot\sum_i (z_{i+1} - z_i)\cdot(w_i + w_{i+1})\cdot(e(\bar{v}_i) + e(\bar{v}_{i+1}))\right]^2\Bigg\}^{1/2} \end{aligned} \tag{31}$$

At Chievo Dam, the uncertainty of bottom discharge (21) may be estimated by

$$e(Q_{\mathrm{b}}) \quad = \quad \pm Q_{\mathrm{b}}\cdot\sqrt{\frac{e^2(z_1) + e^2(z_{\mathrm{b}})}{(z_1 - z_{\mathrm{b}})^2} + f^2(w) + f^2(\bar{v}_1) + f^2(\mathrm{bottom})} \tag{32}$$

where $f(\mathrm{bottom}) = \pm 10\%$ takes into account deviations from the actual flow behavior near the bottom. The intermediate discharge (22) is expected to be measurable with an uncertainty of

$$
\begin{aligned}
e(Q_{\text{int}}) &= \pm\left\{\left[\frac{e^2(z_p)+e^2(z_1)}{(z_p-z_1)^2}\cdot Q_{\text{int}}^2\right]+(f(w)\cdot Q_{\text{int}})^2\right. \\
&\quad \left.+\left[\frac{w}{2}\cdot\sum_i(z_{i+1}-z_i)\cdot(e(\bar{v}_i)+e(\bar{v}_{i+1}))\right]^2\right\}^{1/2} \qquad (33)
\end{aligned}
$$

The uncertainty of surface discharge (23) yields approximately

$$
e(Q_{\text{s}}) = \pm Q_{\text{s}}\cdot\sqrt{\frac{e^2(z_{\text{s}})+e^2(z_p)}{(z_{\text{s}}-z_p)^2}+f^2(w)+f^2(\bar{v}_p)+f^2(\text{surface})} \qquad (34)
$$

where $f(\text{surface}) = \pm 10\%$ takes into account deviations from the actual flow behavior near the water surface. Finally, the uncertainty of the total flow (20) yields

$$
e(Q) \cong \pm\sqrt{e^2(Q_{\text{b}})+e^2(Q_{\text{int}})+e^2(Q_{\text{s}}+(f(\text{conditions})\cdot Q)^2)} \qquad (35)
$$

The available conditions for the ATT measurements at Chievo Dam are considered by $f(\text{conditions}) = \pm 2\%$. This value should cover any local flow effects (vortices, protrusion, ...) whose impact on the results can not be quantified.

Results

Two (2) of the 48 sensors did not work. Hence, the missing plane velocities are obtained by interpolating values from the neighboring paths.
We get a good coincidence when comparing measurements with predicted values. The calculations for different gross heads revealed quite constant expectation values of flow between 50.7 m^3/s and 55.2 m^3/s with an average uncertainty of $\pm 2.3\%$. Figure 6(b) shows the individual flow profiles hereunto. The profile develops a bigger bulge at lower water levels. Interesting profiles of a single measuring point are depicted in figure 6(a). One can observe the existence of a strong main cross flow to the left-hand side. This phenomenon affects the individual flow profiles of the acoustic measuring planes. Using only one acoustic plane would bring drastical underestimation (plane 1–2) or overestimation (plane 3–4) of the total discharge.

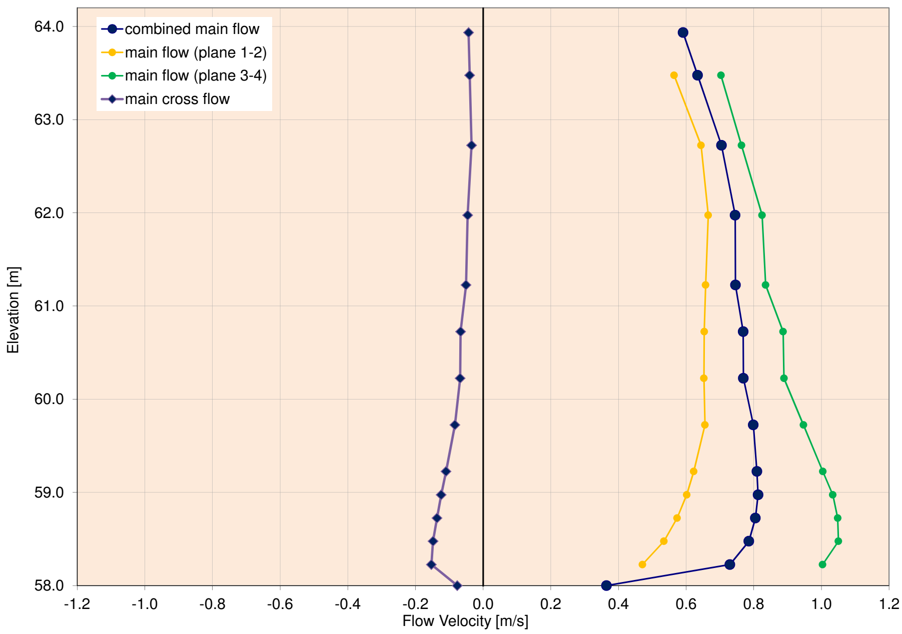

(a) Flow profile at maximum headwater level: cross flow $\bar{v}_\perp$ (blue diamonds), main axial flow $\bar{v}$ (blue circles), axial flow obtained by plane 1–2 v_1 (yellow), and axial flow obtained by plane 3–4 v_2 (green)

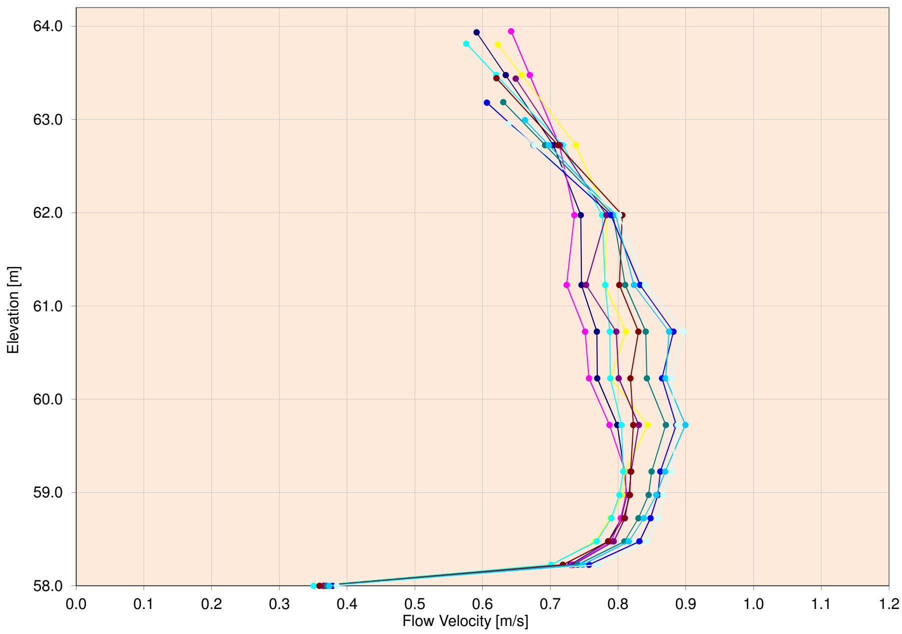

(b) Main axial velocity profiles of different headwater levels: The total discharge remains quite constantly over the whole operating range. Only the profile is getting bulgier with lower head.

Figure 6: Velocity profiles at 5 TG units operation

Discussion

Alignment of sensor pairs

The flow reading started immediatly after turning on the processor unit. The fact that the ultrasonic pulse detection went that well without accurate alignment of the sensor pairs happened to be quite unexpected. The emitters required higher amplification of the pulse. That is reasonable and it was expected. But the most important conclusion can be drawn from the fact, that expensive sensor alignment works done by specialized divers can be avoided in similar cases like at Chievo Dam. It is necessary to take care of the sensor's working frequency, because higher frequencies tend to narrow the angle of aperture.

Uncertainty of the main flow velocity

According to equation (29) the *random* proportion obtained by the regression analysis has to be added to the total uncertainty of the axial flow velocity $e(\bar{v})$. But the unfavorable flow conditions affect heavily the regression parameters and, with this, their uncertainties. Hence, the calculations reveal typical uncertainty values for the regressor $\bar{v}$ of $\pm 5000\%$ (!). This enormous value may be explained by either of the subsequent statements:

1. The normal equations (equations 4 to 7) can not describe the physical behavior of the flow and, therefore, they do not have any significance from a statistical point of view.
2. The normal equations are applied on only one single measuring point, i.e. only the expectation values of the transit times are used what results in 4 equations for 3 unknown parameters (c, $\bar{v}$, $\bar{v}_\perp$). In using n observations the system would contain $4 \cdot n$ equations. The uncertainty analysis could give more plausible values with this proceeding.
3. The complete regression analysis makes no sense for such unfavorable flow conditions.

The author's opinion is that only the second statement can be considered as plausible. Setting up the normal equations as described above yields

$$\mathbf{y} = \mathbf{A} \cdot \mathbf{x} \tag{36}$$

with

$$\mathbf{y} = \begin{pmatrix} \frac{L_1}{t_{1-2}(1)} & \frac{L_1}{t_{2-1}(1)} & \frac{L_2}{t_{3-4}(1)} & \frac{L_2}{t_{4-3}(1)} & \cdots & \frac{L_1}{t_{1-2}(n)} & \frac{L_1}{t_{2-1}(n)} & \frac{L_2}{t_{3-4}(n)} & \frac{L_2}{t_{4-3}(n)} \end{pmatrix}^T \tag{37}$$

$$\mathbf{A} = \begin{pmatrix} 1 & -\cos\theta_1 & -\sin\theta_1 \\ 1 & +\cos\theta_1 & +\sin\theta_1 \\ 1 & -\cos\theta_2 & +\sin\theta_2 \\ 1 & +\cos\theta_2 & -\sin\theta_2 \\ \vdots & \vdots & \vdots \\ 1 & -\cos\theta_1 & -\sin\theta_1 \\ 1 & +\cos\theta_1 & +\sin\theta_1 \\ 1 & -\cos\theta_2 & +\sin\theta_2 \\ 1 & +\cos\theta_2 & -\sin\theta_2 \end{pmatrix} \tag{38}$$

$$\mathbf{x} = \begin{pmatrix} c & \bar{v} & \bar{v}_\perp \end{pmatrix}^T \tag{39}$$

Doing the regression analysis straight forwardly yields to a typical *random* uncertainty of $e_\mathrm{r}(\bar{v}) = \pm 30\%$. This result is still abnormally high, but nevertheless is explainable by bad flow conditions. Anyhow, it gives the possibility to quantify the required number of observations n_min with respect to the choice of a maximum relative random uncertainty $f_{\mathrm{r,max}}$:

$$n_\mathrm{min} = n \cdot \left(\frac{f_\mathrm{r}}{f_{\mathrm{r,max}}}\right)^2 = n \cdot \left(\frac{e_\mathrm{r}(\bar{v}) \cdot \bar{v}}{f_{\mathrm{r,max}}}\right)^2 \tag{40}$$

For Chievo Dam, a single measuring point would have required 90,000 observations to reduce the random uncertainty to $\pm 1\%$. That would have taken 75 hours per measuring point.
As a consequence of this, the contribution of the random uncertainty to the total uncertainty of the main flow velocity is omitted in the results of the Chievo Dam measurements. The regression analysis reveals qualitatively that the inflow conditions were not favorable in the measuring section. The consideration of an additive uncertainty of $f(\text{conditions}) = \pm 2\%$ is therefore an appropriate way. Without such an additive parameter, the average uncertainty of the total flow would be approximately $\pm 0.95\%$ by using common uncertainty propagation. This value is too low – in the author's opinion – in presence of such conditions which were available at Chievo Dam.

Conclusion

- Discharge measurements were carried out on the HYDROMATRIX® module at Chievo Dam using ATT method.
- It turned out that the pre-alignment of transducer pairs on the frames (fixation to a distinct angles) was sufficient outside the channel. Accurate alignment at mounted positions on the side walls were not necessary due to the pulse emission characteristics of the sensors.
- The average uncertainty of the total flow is estimated to be $\pm 2.3\%$ considering the available, unfavorable flow conditions and the application of 24 acoustic paths.

- A criterion to quantify the required number of observations (samples) is introduced which is based on a test sample and the choice of the maximum allowable random uncertainty.

Vitae

Johannes Lanzersdorfer graduated in Technical Physics from the Technical University of Graz in 2008. He is working at ANDRITZ Hydro in Linz as a measurement engineer since 2009. His field of activity includes field measurements and the development of measuring techniques for the hydraulic laboratory and for field testing.

References

[1] IEC 60041, editor. *Field acceptance tests to determine the hydraulic performance of hydraulic turbines, storage pumps and pump-turbines*. IEC, 3 edition, 1991.

[2] ISO 6416, editor. *Hydrometry – Measurement of discharge by the ultrasonic (acoustic) method*. ISO, 3 edition, 1994.

[3] *Accusonic 7500 Series Flowmeter - Technical Reference Manual*. http://www.accusonic.com/.

[4] Technical advice by Accusonic.

[5] Irene A. Stegun Milton Abramowitz. *Handbook of mathematical functions*. Dover Publications, 2000.